JCB Article

Stu2p, the budding yeast member of the conserved Dis1/XMAP215 family of microtubule-associated proteins is a plus end–binding microtubule destabilizer

Mark van Breugel, David Drechsel, and Anthony Hyman

Max Planck Institute of Molecular Cell Biology and Genetics, 01307 Dresden, Germany

The Dis1/XMAP215 family of microtubule-associated proteins conserved from yeast to mammals is essential for cell division. XMAP215, the *Xenopus* member of this family, has been shown to stabilize microtubules in vitro, but other members of this family have not been biochemically characterized. Here we investigate the properties of the *Saccharomyces cerevisiae* homologue Stu2p in vitro. Surprisingly, Stu2p is a microtubule destabilizer that binds preferentially to microtubule plus ends. Quantitative analysis of microtubule dynamics suggests that Stu2p induces microtubule catastrophes by sterically interfering with tubulin addition to microtubule ends. These results reveal both a new biochemical activity for a Dis1/XMAP215 family member and a novel mechanism for microtubule destabilization.

Introduction

Microtubules are semirigid tube-like polymers built up from tubulin subunits composed of a 1:1 heterodimer of α- and β-tubulin. Microtubules in vitro and in vivo show an assembly property known as dynamic instability in which microtubule ends stochastically switch from states of growing to shrinking (an event called catastrophe) and from shrinking to growing (an event called rescue). Microtubule polarity is reflected in the difference in polymerization dynamics at the two ends, with the plus end growing faster than the minus end (for review see Desai and Mitchison, 1997).

Although dynamic instability is an intrinsic property of microtubules growing in vitro from pure tubulin, there are significant differences in the dynamic properties of microtubules in vitro and in vivo. For a given concentration of tubulin, the growth rate and the catastrophe frequency are much higher in vivo than in vitro. Furthermore, the growth rate and the catastrophe frequency of microtubules vary both during development and through the cell cycle. Thus, it is thought that microtubule dynamics in vivo are influenced by additional cellular factors (for reviews see Desai and Mitchison, 1997; Kinoshita et al., 2002). Such factors can be roughly placed in one of two functional families: those that promote microtubule assembly, such as XMAP215, tau, or MAP4, and those that inhibit microtubule assembly, such as members of the KinI family, Op18/Stathmin, or katanin. The mechanisms by which microtubule stabilizers and destabilizers modulate microtubule dynamics are different. Neuronal microtubule-associated proteins like tau, MAP1, or MAP2 are thought to cross-link adjacent tubulin subunits along the microtubule lattice and thereby suppress microtubule destabilization (for review see Desai and Mitchison, 1997). Other microtubule-associated proteins such as EB1 or CLIPs bind to microtubule ends where they directly or indirectly stabilize microtubules by acting as anticatastrophe factors (Brunner and Nurse, 2000; Akhmanova et al., 2001; Nakamura et al., 2001; for review see Schuyler and Pellman, 2001). Some destabilizers such as Op18/Stathmin work by sequestering free tubulin or through directly modulating microtubule structure (Belmont and Mitchison, 1996; Curmi et al., 1997; Jourdain et al., 1997; Howell et al., 1999). Others such as the KinI family of destabilizers or katanin require the energy of ATP hydrolysis to destabilize microtubules (McNally and Vale, 1993; Desai et al., 1999).

Recently, one family of essential microtubule stabilizers, the Dis 1/TOG family, has emerged as a putative master regulator of microtubule dynamicity (for reviews see Ohkura et al., 2001; Kinoshita et al., 2002). Members have been found in every organism where investigated, and it is currently the only known family of microtubule-associated proteins common to plants, fungi, and animals. XMAP215, from *Xenopus laevis*, is the best studied member of this family (Gard and Kirschner, 1987; Vasquez et al., 1994; Tournebize et al.,

The online version of this article includes supplemental material.

Address correspondence to Anthony Hyman, Max Planck Institute of Molecular Cell Biology and Genetics, Pfotenhauerstrasse 108, 01307 Dresden, Germany. Tel.: 49-351-210-1280. Fax: 49-351-210-1289. E-mail: hyman@mpi-cbg.de

*Abbreviations used in this paper: HU, hydroxyurea; VE-DIC, video-enhanced differential interference contrast microscopy.

Key words: microtubule; dynamics; assembly; XMAP215; Dis1

The Journal of Cell Biology, Volume 161, Number 2, April 28, 2003 359–369
http://www.jcb.org/cgi/doi/10.1083/jcb.200211097

2000; Cassimeris et al., 2001; Kinoshita et al., 2001; Popov et al., 2001, 2002). In cytoplasmic egg extracts, XMAP215 stabilizes microtubules primarily by antagonizing the activity of the microtubule destabilizer XKCM1, a member of the KinI family (Tournebize et al., 2000). Thus, immunodepletion of XMAP215 decreases the steady-state length of microtubules. Similarly, *zyg-9* mutants in *Caenorhabditis elegans* (Matthews et al., 1998) and *msps* mutants in *Drosophila* also seem to decrease the steady-state length of microtubules (Cullen et al., 1999; Lee et al., 2001). Together, these studies suggest an evolutionarily conserved role of this family in stabilizing microtubules. However, analyses of Stu2p, the *Saccharomyces cerevisiae* member of this family, have complicated the general conclusion that proteins from this family are microtubule stabilizers. In in vivo, run-down experiments strongly reduced Stu2p levels lead to less dynamic microtubules, with a lower catastrophe frequency (Kosco et al., 2001). These results suggest that the role of Stu2p in yeast is to destabilize microtubules. On the other hand, a more indirect study showed Stu2p to be required for spindle elongation (Severin et al., 2001).

It is unclear whether this difference in activity between the *S. cerevisiae* and the *Xenopus* members of the family represent fundamental differences in the biochemical properties of the proteins or whether the proteins are acting in different cellular contexts. The stabilizing activity of XMAP215 in vivo is reflected in its effect on microtubule dynamics in vitro where it acts as a microtubule stabilizer: when added to pure tubulin, XMAP215 stimulates the plus end growth rate 7–10-fold (Gard and Kirschner, 1987; Vasquez et al., 1994). However, the biochemical activity of Stu2p on purified tubulin growing in vitro has not been measured.

Results

To investigate the biochemical activities of Stu2p, we sought to make pure recombinant protein. Stu2p has previously been expressed in reticulate lysates (Wang and Huffaker, 1997), but the amounts obtained were too small for tubulin-dependent assays. Although *Escherichia coli*–expressed Stu2p is apparently soluble, it aggregated in the presence of microtubules (unpublished data). Therefore, we expressed and purified Stu2p using recombinant baculovirus. Typically, a 500-ml insect cell culture yielded 4 mg protein that was over 90% pure (Fig. 1 A).

To characterize the recombinant Stu2p, we determined its Stokes radius using gel filtration on a Superose 6 column. Fig. 1 B (top) shows a Western blot of the collected fractions of the Stu2p run. Arrows indicate the position of marker proteins used to calibrate the column. Stu2p exhibited a symmetric peak, and none was found in the void volume of the column, confirming that the recombinant protein is soluble. From these data, we derived a Stokes radius of 11.1 nm for the recombinant Stu2p. To compare the Stokes radius of the recombinant Stu2p with endogenous Stu2p, yeast extracts were run on the same gel filtration column and Stu2p was monitored by Western blotting (Fig. 1 B, bottom). The Stokes radius of endogenous Stu2p was found to be ~12.3 nm. Thus, the Stokes radius of endogenous and recombinant Stu2p can be considered almost identical given the very different nature of pure recombinant proteins and yeast extracts. Such high Stokes radii suggest that Stu2p forms a homomultimer, is a very elongated molecule, or both. To differentiate between these possibilities, we obtained the S value of Stu2p using sucrose gradients. Recombinant Stu2p or yeast extracts were spun through a linear 5–40% sucrose gradient. Fig. 1 C shows the Western blot for recombinant Stu2p (top) and for yeast extracts (bottom). From these gradients, we derived an apparent S value for both endogenous and recombinant Stu2p of 4.6. Combining S value and Stokes radius provides a native molecular weight of 199.6 kD for the recombinant and 221.2 kD for the endogenous Stu2. Since the calculated molecular weight of Stu2p is 100.9 kD, this suggests that it forms a stable dimer in solution. We confirmed that Stu2p forms a stable complex with itself in vivo by coimmunoprecipitating endogenous Stu2p together with enhanced GFP (EGFP)*-

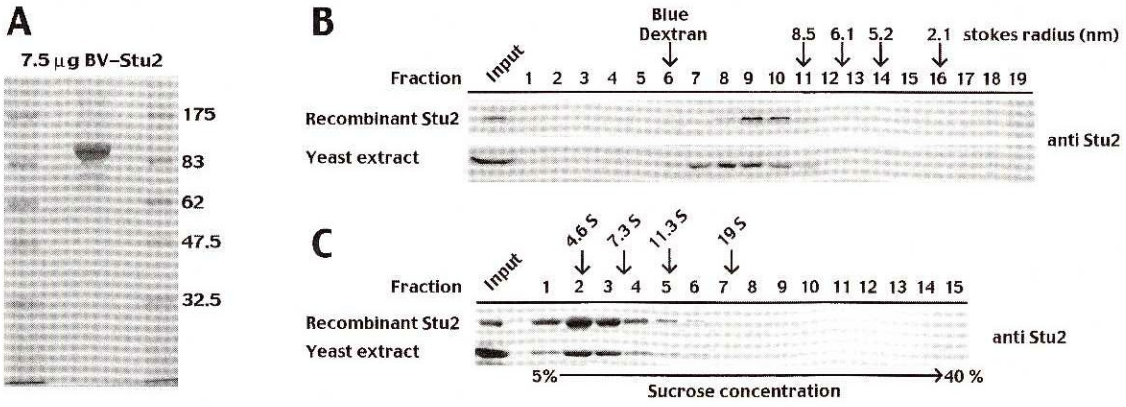

Figure 1. **Recombinant, baculovirus-derived Stu2p and endogenous Stu2p show similar hydrodynamic properties.** (A) Coomassie blue–stained SDS-polyacrylamide gel showing ~7.5 µg of purified, baculovirus-derived Stu2p. (B) Determination of the Stokes radius of baculovirus-derived and endogenous Stu2p in yeast extracts using gel filtration on a Superose 6 column. The fractions with recombinant Stu2p (top) or yeast extract (bottom) were separated by SDS-PAGE, and Stu2p was detected by Western blotting using a polyclonal Stu2p antibody. The corresponding positions of selected markers of known Stokes radius are indicated by arrows. (C) Determination of the S value of recombinant and endogenous Stu2p in yeast extracts. Recombinant Stu2p and endogenous Stu2p in yeast extracts were spun through a linear 5–40% sucrose gradient. Fractions were analyzed by SDS-PAGE and Western blotting using a polyclonal Stu2p antibody. (Top) Western blot for recombinant Stu2p; (bottom) Western blot for endogenous Stu2p. Corresponding positions of markers with known S value are indicated by arrows.

tagged Stu2p in yeast extracts (Fig. S1, available at http://www.jcb.org/cgi/content/full/jcb.200211097/DC1). Therefore, we conclude that in contrast to Stu2p, XMAP215, its *Xenopus* homologue, remains monomeric in solution (Gard and Kirschner, 1987; Cassimeris et al., 2001). Furthermore, Stu2p has a very high Stokes radius for a protein of 200 kD. A globular protein of this size would be expected to have a Stokes radius of ~5 nm. Thus, like XMAP215 (Gard and Kirschner, 1987; Cassimeris et al., 2001), the Stu2p dimer has a very elongated shape.

Many microtubule-associated proteins like MAP1, MAP2, and tau (Serrano et al., 1985), but not the human Stu2p homologue ch-TOG (Spittle et al., 2000), require the COOH-terminal tail of β-tubulin for microtubule binding. To determine the involvement of the β-tubulin COOH terminus in binding of Stu2p to microtubules, we made microtubules without the COOH terminus by limited subtilisin proteolysis of taxol-stabilized microtubules. Fig. 2 A shows a Coomassie-stained gel of mock-digested and digested microtubules and a Western blot probed with an antibody specific for the COOH terminus of β-tubulin. We determined the relative extent of binding of Stu2p to these microtubules by incubating increasing amounts of them with 18 nM Stu2p at room temperature. Bound Stu2p was separated from unbound Stu2p by centrifugation, supernatants and pellets were analyzed by Western blotting (Fig. 2 B), and the extent of binding was subsequently quantitated (Fig. 2 C). Over a wide concentration range of microtubules, Stu2p bound to a similar extent to the undigested and the digested microtubules. Thus, Stu2p, like its human homologue ch-TOG but unlike many other microtubule-associated proteins so far studied, does not seem to have a strong requirement of the COOH terminus of β-tubulin for microtubule binding.

We tested the effects of recombinant Stu2p on the length of microtubules growing in vitro from purified centrosomes using rhodamine tubulin to monitor microtubule length. Microtubule growth was initiated at 29°C at 26 μM tubulin in the presence of increasing amounts of Stu2p. After 10 min, the reactions were fixed, quenched, and analyzed microscopically. Fig. 3 A shows a representative aster for each tested Stu2p concentration, and Fig. 3 B is a plot of the aster size distribution at the different Stu2p concentrations. Stu2p addition was found to lead to a clear reduction in microtubule length. This effect starts at 0.1 μM Stu2p and saturates below 0.33 μM. Thus, we conclude that Stu2p acts to destabilize microtubules in vitro.

To further confirm that Stu2p can act in vivo as a destabilizer of cytoplasmic microtubules, we used the temperature-sensitive mutant stu2–10 to abolish Stu2p function (Severin et al., 2001). To avoid complications from a stu2–10–dependent cell cycle arrest (Severin et al., 2001), we arrested both wild-type and stu2–10 cells in S phase at the permissive temperature with hydroxyurea (HU). After HU arrest, the cultures were shifted to 37°C, and the length of cytoplasmic microtubules were determined. Fig. 4 A shows a FACS® analysis of the cells throughout the experiment, demonstrating a complete cell cycle block at S phase. Fig. 4 B shows a projected antitubulin immunofluorescence of wild-type or stu2–10 cells arrested in HU at the permissive temperature before (top) or after the shift to the restrictive temperature (bottom and representative close ups in Fig. 4 C). Fig. 4 D shows the respective length distribution of cytoplasmic microtubules, and Fig. 4 E shows the average cytoplasmic microtubule lengths. Very similar in length before the tempera-

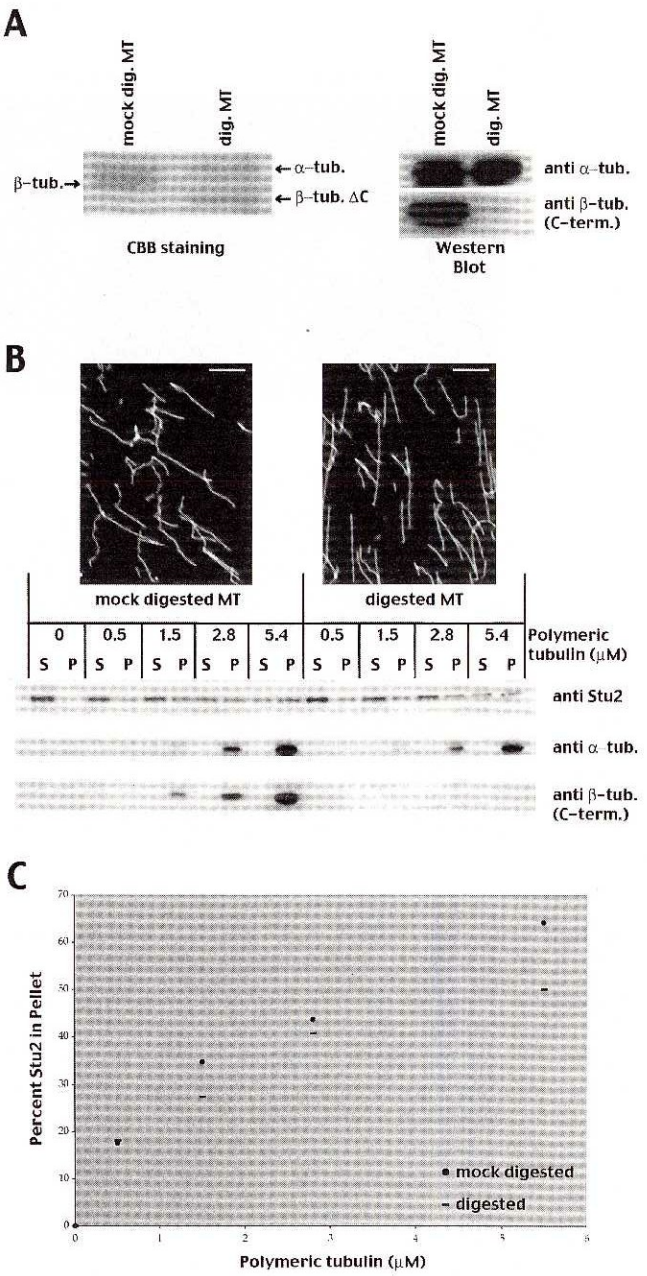

Figure 2. **Stu2p does not strongly require the COOH terminus of β-tubulin for binding to microtubules.** (A) Mock- or subtilisin-digested microtubules analyzed by SDS-PAGE and Coomassie blue staining (left) or by Western blotting (right) using a monoclonal α-tubulin antibody (top) or a monoclonal β-tubulin antibody whose epitope lies within the COOH terminus of β-tubulin (bottom). (B, top) Mock- and subtilisin-digested microtubules visualized by immunofluorescence. Bar, 5 μm. (B, bottom) Increasing amounts of mock- or subtilisin-digested microtubules were incubated with 18 nM Stu2p and bound separated from unbound Stu2p by centrifugation. Equivalent amounts of the supernatants (S) and the pellets (P) were analyzed by SDS-PAGE and Western blotting using a polyclonal Stu2p antibody (top), a monoclonal α-tubulin antibody (middle), or a monoclonal β-tubulin antibody whose epitope lies within the COOH terminus of β-tubulin (bottom). (C) Plot showing the percentage of Stu2p bound to mock- or subtilisin-digested microtubules at different microtubule concentrations.

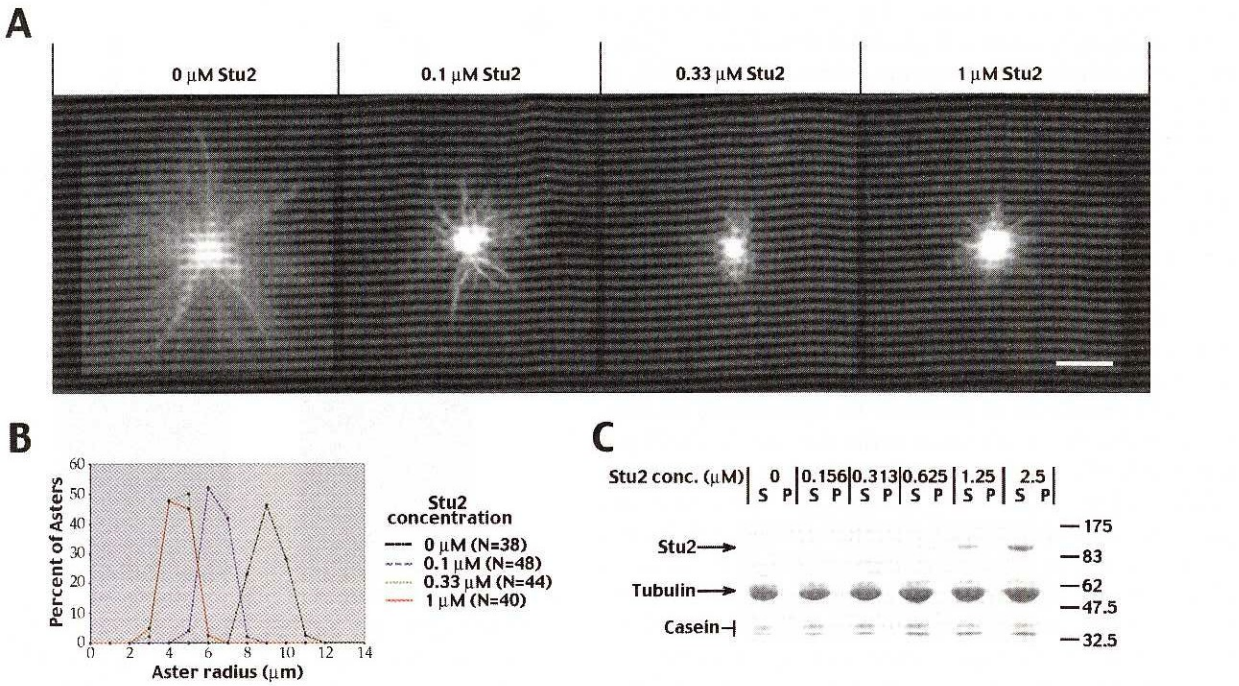

Figure 3. **Stu2p decreases microtubule length in vitro.** (A) Microtubule asters at increasing Stu2p concentrations visualized by incorporation of rhodamine tubulin. Shown are representative examples of asters at 0, 0.1, 0.33, and 1 μM Stu2p. Bar, 4 μm. (B) Plot showing the distribution of aster radii at each Stu2p concentration. (C) Stu2p does not cause spontaneous tubulin nucleation in solution. Increasing amounts of Stu2p were incubated with 22 μM tubulin for 10 min at 29°C. Reactions were spun through a 40% glycerol cushion, and equivalent amounts of supernatants (S) and pellets (P) were analyzed by SDS-PAGE and Coomassie blue staining.

ture shift (wild type, 1.03 ± 0.07 [SEM; $p < 0.05$]) μm; stu2–10, 1.07 ± 0.07 μm), the length of cytoplasmic microtubules of stu2–10 and wild-type cells increases after the shift to the restrictive temperature (Fig. 4, D and E), reflecting the effect of the higher temperature and the larger cell size (see Materials and methods). However, after the temperature shift cytoplasmic microtubules of stu2–10 cells are on average ~30% longer than the ones of wild-type cells (wild-type, 1.70 ± 0.13 μm; stu2–10, 2.29 ± 0.20 μm) (Fig. 4, D and E). Thus, Stu2p can act as a microtubule destabilizer in vivo and in vitro.

We wanted to further understand the mechanism by which Stu2 destabilizes microtubules. Stu2p could destabilize microtubules by inhibition of growth rate, promotion of microtubule shrinkage rate, through induction of catastrophes or prevention of rescues. To distinguish between these possibilities, we used video-enhanced differential interference contrast microscopy (VE-DIC). Microtubules were nucleated from purified centrosomes adsorbed to the coverslips of small perfusion chambers. Fig. 5 A shows three typical microtubule traces for three different Stu2p concentrations. Fig. 5 B shows the average growth rate, Fig. 5 C shows the catastrophe rate, and Fig. 5 D displays the average shrinkage rate as a function of Stu2p concentration. These data are summarized in Fig. 5 E. Rescue events occurred too rarely to make a statement about Stu2p's influence on the rescue frequency. Stu2p has a very minor effect on microtubule shrinkage rate that is only seen at high Stu2p concentrations. In contrast, Stu2p shows a marked inhibition of microtubule growth rate that starts at very low concentrations (0.03 μM) and begins to saturate at ~0.1 μM. Similarly, Stu2p shows a marked promotion of catastrophes that begins at 0.03 μM and saturates at ~0.1 μM. Thus, Stu2p destabilizes microtubules by decreasing their growth rate and increasing their catastrophe rate. This is in direct contrast to its *Xenopus* homologue XMAP215 that under very similar buffer conditions in vitro acts as a microtubule stabilizer (Vasquez et al., 1994; Kinoshita et al., 2001).

We wondered whether the stimulation of catastrophes by Stu2p was a direct effect on the catastrophe rate or indirectly caused by its inhibition of microtubule growth rate. To test this we first obtained the relation between microtubule growth rate and catastrophe frequency in the absence of Stu2p under our buffer conditions. We recorded microtubule growth at different tubulin concentrations using VE-DIC, binned the microtubule traces according to their growth rates, and calculated the corresponding catastrophe frequencies. The graph is shown in Fig. 5 F (varying tubulin). In agreement with published data (Drechsel et al., 1992), the catastrophe frequency increases asymptotically with decreasing growth rate. To this plot we added the growth rate catastrophe frequency values of the experiment in the presence of Stu2p (Fig. 5 F, varying Stu2p). At each given growth rate of microtubules in the presence of Stu2p the corresponding catastrophe frequency is almost identical to the one at a similar growth rate in the absence of Stu2p. Thus, Stu2p probably promotes microtubule catastrophes by inhibiting the microtubule growth rate.

Microtubule-associated proteins are known to be strong microtubule nucleators under certain conditions as shown re-

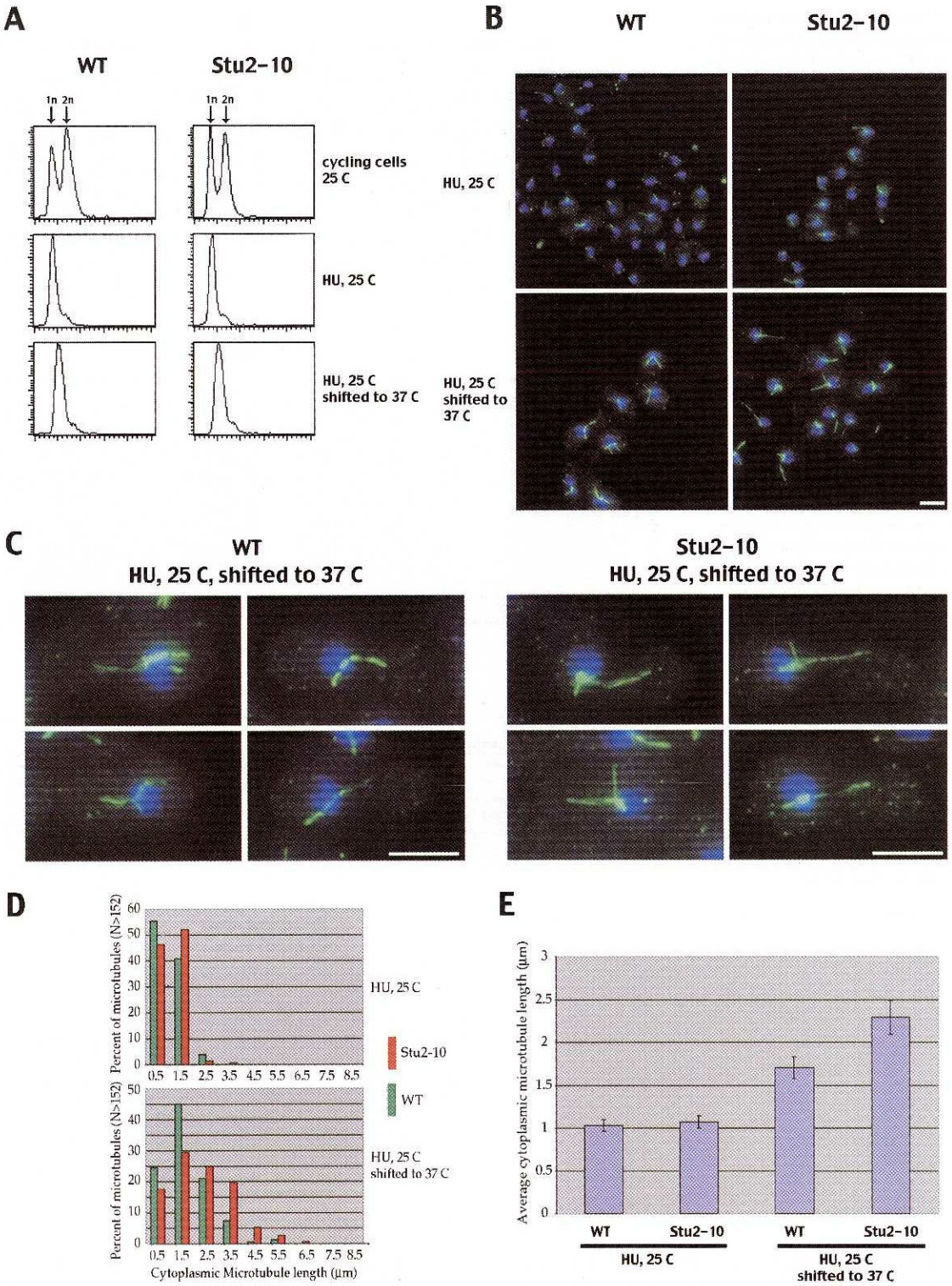

Figure 4. **Stu2p can destabilize cytoplasmic microtubules in vivo.** Wild-type or stu2–10 cells were HU arrested at the permissive temperature, shifted to the restrictive temperature, and the cytoplasmic microtubule length was determined by indirect immunofluorescence and three dimensional tracking. (A) FACS® profiles of cycling wild-type or stu2–10 cells at 25°C (top) that were arrested at 25°C with HU before (middle) or after shifting the cells to 37°C (bottom). (B) Projected indirect antitubulin immunofluorescence of wild-type or stu2–10 cells arrested at 25°C with HU before (top) or after shifting the cells to 37°C (bottom). Green, microtubules; blue, DNA. Bar, 5 μm. (C) Projected indirect antitubulin immunofluorescence of wild-type (left) or stu2–10 cells (right) arrested at 25°C with HU after shifting the cells to 37°C. Close-ups of four representative cells. Green, microtubules; blue, DNA. Bar, 5 μm. (D) Length distribution (in 1-μm intervals) of cytoplasmic microtubules of wild-type and stu2–10 cells arrested at 25°C with HU before (top) or after shifting the cells to 37°C (bottom). Green, wild-type microtubules; red, stu2–10 microtubules. (E) Average length of cytoplasmic microtubules of wild-type or stu2–10 cells arrested at 25°C with HU before and after shifting the cells to 37°C. Error bars represent SEM ($P < 0.05$).

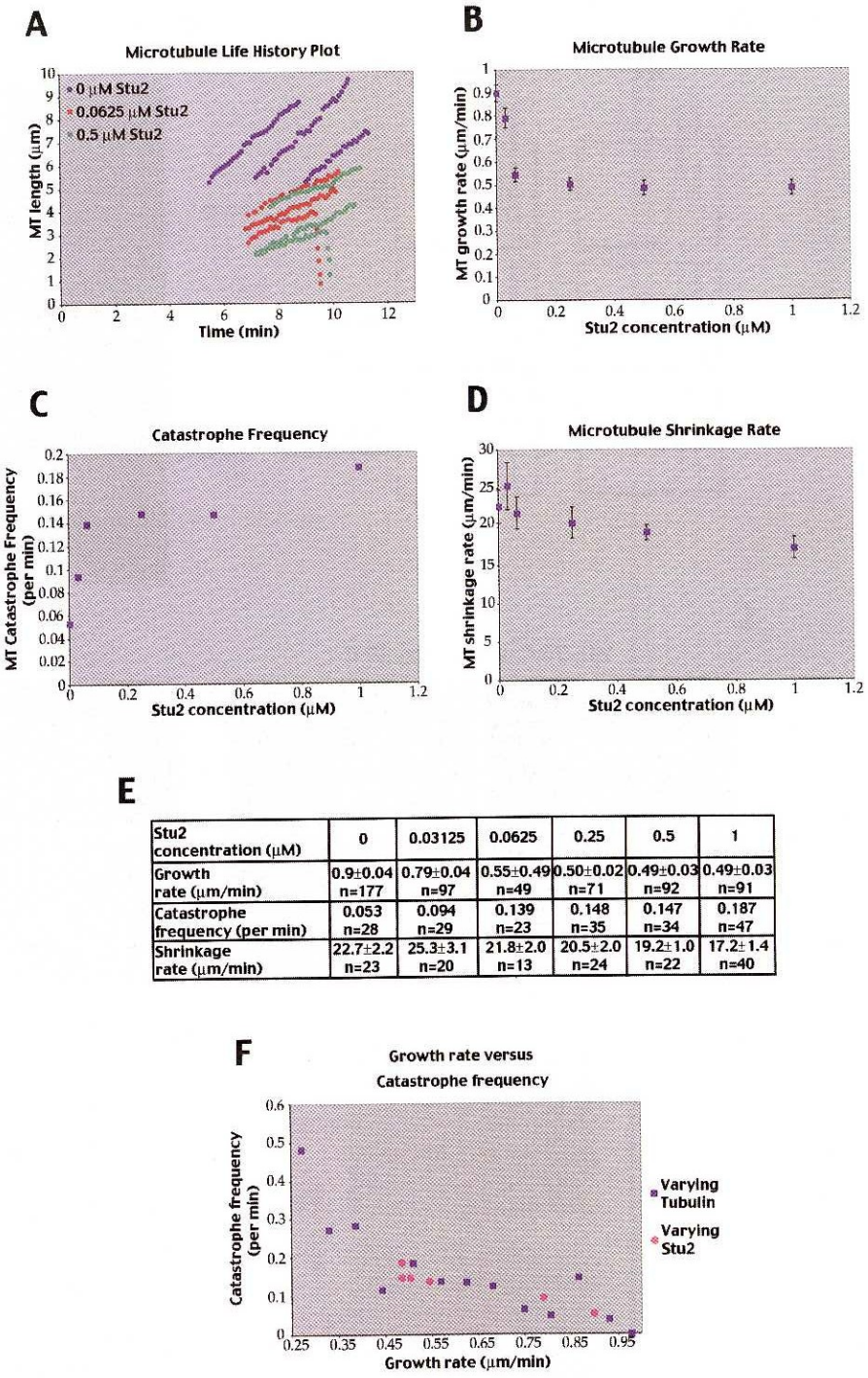

E

Stu2 concentration (μM)	0	0.03125	0.0625	0.25	0.5	1
Growth rate (μm/min)	0.9±0.04 n=177	0.79±0.04 n=97	0.55±0.49 n=49	0.50±0.02 n=71	0.49±0.03 n=92	0.49±0.03 n=91
Catastrophe frequency (per min)	0.053 n=28	0.094 n=29	0.139 n=23	0.148 n=35	0.147 n=34	0.187 n=47
Shrinkage rate (μm/min)	22.7±2.2 n=23	25.3±3.1 n=20	21.8±2.0 n=13	20.5±2.0 n=24	19.2±1.0 n=22	17.2±1.4 n=40

Figure 5. **Stu2p induces catastrophes by decreasing microtubule growth rate.** Real-time VE-DIC analysis of microtubules in the presence of increasing amounts of Stu2p. (A) Three examples of traces of individual microtubules at 0, 62.5, and 500 nM Stu2p. (B) Stu2p inhibits microtubule growth rate. A plot showing the averaged growth rates of microtubules at different concentrations of Stu2p. Error bars represent the SEM ($P \leq 0.05$). (C) Stu2p increases microtubule catastrophe frequency. A plot showing the microtubule catastrophe frequency at different concentrations of Stu2p. (D) Stu2p decreases microtubule shrinkage rate. A plot showing the averaged shrinkage rates of microtubules at different concentrations of Stu2p. Error bars represent the SEM ($P \leq 0.05$). (E) The derived dynamic parameters of microtubule polymerization in the presence of increasing amounts of Stu2p. The rescue frequency could not be determined. (F) Stu2p does not directly stimulate microtubule catastrophes. A plot showing the microtubule growth rate catastrophe frequency relation in pure tubulin (varying tubulin). The growth rates and corresponding catastrophe frequencies with varying amounts of Stu2p (as summarized in E) were added to this plot. Growth rate and corresponding catastrophe frequency at increasing concentrations of pure tubulin were obtained by VE-DIC, individual microtubule traces were binned in 0.06 μm/min growth rate intervals, and the catastrophe frequency in each interval was calculated subsequently.

cently for XMAP215 (Popov et al., 2002). One possibility is that the decreased growth rate could result from a reduction in the free tubulin pool due to nucleation of noncentrosomal microtubules by Stu2p. To test the nucleation ability of Stu2p, we mixed Stu2p and tubulin in the absence of centrosomes and recovered nucleated microtubules by centrifugation. 22 μM tubulin was incubated with increasing amounts of Stu2p for 10 min at 29°C. The reactions were spun through a 40% glycerol cushion at 29°C, and supernatant and pellet were analyzed by SDS-PAGE and Coomassie staining. No significant nucleation was seen over the wide concentration range of Stu2p tested (Fig. 3 C). In agreement, we observed no spontaneously nucleated microtubules in the VE-DIC assays (unpublished data). Thus, we believe that the destabilization of microtubules is a direct effect of Stu2p on microtubule dynamics and not an indirect effect on the effective tubulin concentration available for polymerization.

How does Stu2p inhibit microtubule growth? Interestingly, the inhibition of the microtubule growth rate by Stu2p saturated at relatively low Stu2p concentrations (~0.1 μM Stu2p with 21.5 μM tubulin in the VE-DIC assay, below 0.33 μM Stu2p with 26 μM tubulin in a fixed time point assay). Mechanistically, that argues in favor of a model in which a limited number of microtubule-binding sites nec-

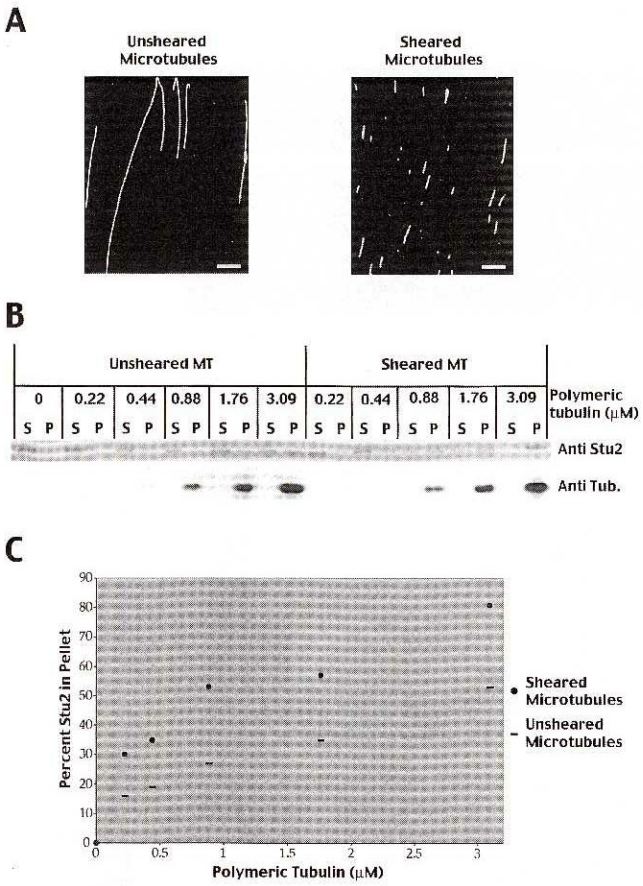

Figure 6. **Stu2p binds preferentially to microtubule ends.** (A) Anti-tubulin immunofluorescence of taxol stabilized microtubules before and after shearing with a tip sonicator. Bar, 5 μm. (B) Stu2p binds to a higher extent to sheared microtubules. Increasing amounts of unsheared or sheared microtubules were incubated with 19 nM Stu2p, and bound Stu2p separated from unbound Stu2p by centrifugation. Equivalent amounts of supernatants (S) and pellets (P) were analyzed by SDS-PAGE and Western blotting using a polyclonal Stu2p antibody (top) or a monoclonal tubulin antibody (bottom). (C) Plot showing the percentage of Stu2p bound to microtubules at different microtubule concentrations.

essary for efficient growth become preferentially bound and saturated by Stu2p. An obvious location of such sites is the microtubule end. Indeed, there is evidence for Stu2p binding in vivo to MT ends (He et al., 2001; Kosco et al., 2001). Therefore, we determined the relative affinities of Stu2p for microtubule ends versus the lattice. We took advantage of the fact that taxol-stabilized microtubules can be sheared so that the concentration of polymeric tubulin remains constant with a significant increase in the concentration of microtubule ends. If Stu2p binds microtubule ends preferentially, more Stu2p should bind to sheared microtubules. Examples of sheared and unsheared microtubules are shown in Fig. 6 A. Sheared microtubules were on average fivefold shorter then the unsheared microtubules (see Materials and methods). Increasing amounts of microtubules were incubated with 19 nM Stu2p at room temperature. Microtubule-bound Stu2p was separated from unbound Stu2p by centrifugation, and the supernatant and pellet were analyzed by Western blotting. Fig. 6 B shows the Western blot probed for Stu2p and tubulin. Fig. 6 C shows a graph with the percent of microtubule-bound Stu2p plotted against the microtubule concentrations. At each given concentration of microtubules, more Stu2p bound to the sheared than to the nonsheared microtubules. Thus, Stu2p binds preferentially to microtubule ends as opposed to lateral microtubule binding sites. Under less stringent conditions, some end binding has been reported previously in vitro for the human Stu2p homologue ch-TOG (Spittle et al., 2000).

Binding of Stu2p to sheared microtubules is an indirect measurement of the affinity of Stu2p to microtubule ends. To directly visualize Stu2p binding to microtubule ends, we labeled Stu2p with the fluorescent dye Cy3. Cy3-Stu2p was incubated with taxol-stabilized microtubules labeled with Oregon green. To mark the microtubule polarity, the microtubule minus ends were brighter than the plus ends (Fig. 7 A; see Materials and methods). Reactions were fixed, quenched, and analyzed microscopically. Fig. 7 A shows representative Stu2p-bound microtubules. Microtubules are in green, and Stu2p is in red. Stu2p can be seen preferentially at the microtubule plus end. The distribution of Stu2p binding to microtubules was quantified by scanning the intensities of the Stu2p signal along the length of individual microtubules. Signals higher than 10% of the median intensity along the given microtubule were scored with their location. Fig. 7 B shows the distribution of the number of Stu2p spots per microtubule. Fig. 7 C shows a histogram with the frequency at which Stu2p signals are found at 10% distance intervals from the minus end to the plus end of the microtubules. Almost 40% of the Stu2p signals were found at microtubule plus ends. The remainder of the signals are relatively uniformly distributed with a frequency of ~7% per distance interval along the rest of the microtubule, arguing against any preference of Stu2p among these lateral sites. To eliminate the possibility that Stu2p binding to the microtubule minus ends was inhibited by the relatively high levels of labeling there, we made nonpolarity marked microtubules and examined the end binding of Stu2p. Under these conditions as with polarity marked microtubules, ~40% of the microtubules had Stu2p bound to one end only (unpublished data).

Discussion

In this report, we have investigated the activity of Stu2p in vitro and how this activity relates to its known function in vivo. In contrast to the commonly held belief that members of the Dis1/XMAP215 family of microtubule-associated proteins all act to stabilize microtubules, we find that Stu2p is a microtubule destabilizer. Furthermore, we show that Stu2p is to our knowledge unique among the few known microtubule end–binding proteins in recognizing and preferentially binding microtubule plus ends in vitro. Our hydrodynamic analysis shows that Stu2p, like XMAP215, is an elongated molecule. However, in contrast to XMAP215, which is a monomer in solution (Gard and Kirschner, 1987; Cassimeris et al., 2001), Stu2p seems to be a dimer in vitro and in vivo. The real molecular weight of recombinant and endogenous Stu2p is ~200 and ~220 kD, respectively. Given the different nature of yeast extracts and pure proteins, a difference in the derived real molecular weight of 10% is within the exper-

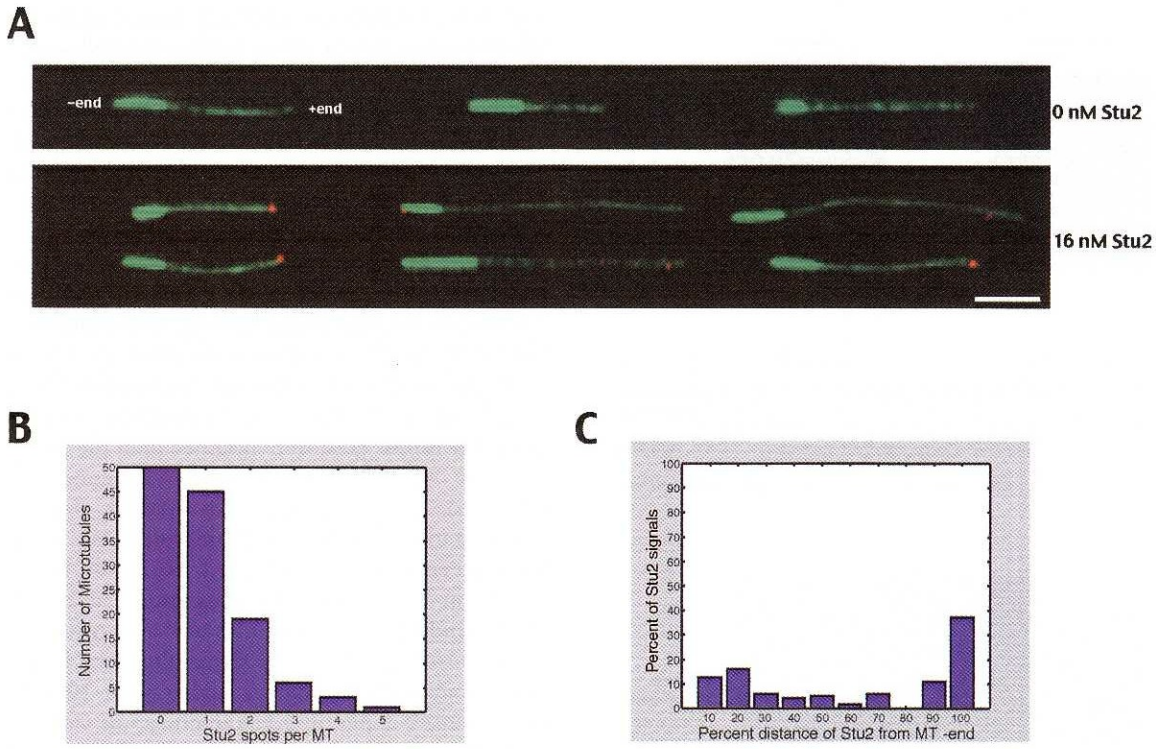

Figure 7. **Stu2p binds preferentially to microtubule plus ends.** Visualization of Stu2p binding to microtubules using directly Cy3-labeled Stu2p and polarity-marked microtubules. Stu2p intensity was scanned in the rhodamine channel from the minus end along the length of microtubules, and signals higher than 10% of the median intensity were scored with their location. (A) Representative examples of polarity-marked microtubules in the absence or in the presence of 16 nM Stu2p. Polarity marked microtubules are in green, and Stu2p is in red. The minus end of microtubules is brighter than the plus end. Bar, 3 μm. (B) Histogram showing the number of Stu2p spots per microtubule. (C) Histogram showing the percentage of Stu2p signals found in 10% intervals from the minus ends of the microtubules to their plus ends.

imental error. Thus, although we cannot rule out that Stu2p might be stably complexed with a small protein of ~20 kD in vivo, we consider this to be unlikely.

The question we set out to answer was whether the difference in activity between the *S. cerevisiae* and the *Xenopus* members of the family in vivo represent fundamental differences in the biochemical properties of the proteins or whether the proteins are acting in different cellular contexts. In vitro, XMAP215 stabilizes microtubules by increasing the growth and shrinkage rate without affecting catastrophe frequency (Gard and Kirschner, 1987; Vasquez et al., 1994). Here we show that in contrast to XMAP215, Stu2p destabilizes microtubules in vitro.

Stu2p constitutes a new class of microtubule destabilizers. The other well-characterized microtubule destabilizers differ from Stu2p in their effect on microtubule dynamics. The KinI family of microtubule destabilizers bind to both plus and minus ends and are thought to trigger catastrophes by bending protofilaments into a structure that is found in a microtubule undergoing a catastrophe (Desai et al., 1999; Moores et al., 2002). They need the energy of ATP hydrolysis to recycle for multiple rounds of action. The destabilizing mechanism of katanin also depends on the hydrolysis of ATP. It disrupts noncovalent bonds between tubulin dimers within the microtubule lattice presumably by preferentially acting on microtubule lattice defects (McNally and Vale, 1993; Davis et al., 2002). Op18/Stathmin stimulates catastrophes directly at tips (Belmont and Mitchison, 1996; Howell et al., 1999) or acts through sequestering tubulin (Curmi et al., 1997; Jourdain et al., 1997; Howell et al., 1999). In contrast, Stu2p does not need energy to operate nor directly promotes catastrophes but rather decreases microtubule growth rate with a resultant increase in catastrophe frequency.

Stu2p's mechanism of destabilization cannot be explained by direct sequestering, given the relative concentrations of Stu2p and tubulin (0.1 and 21.5 μM, respectively) and the saturation of destabilization. How then do the microtubule-binding characteristics of Stu2p relate to its destabilizing activity? We propose that Stu2p destabilizes microtubules by preferentially binding to their plus ends and sterically hindering tubulin addition. This would lead to a decrease in microtubule growth rate, an increased probability of hydrolysis of the stabilizing GTP cap at microtubule plus ends, and an indirect increase in catastrophe frequency. Another possibility is that Stu2p changes the structure of the microtubule end, for instance, by affecting the length of the protofilament sheet characteristic for growing ends (Chretien et al., 1995; Arnal et al., 2000).

How does the in vitro activity of Stu2p relate to its function in vivo? Using a temperature-sensitive allele of Stu2, we were able to show that Stu2p can act in vivo as a microtubule destabilizer as it does in vitro. This is in agreement with an earlier in vivo study (Kosco et al., 2001). Here, using a copper run-down, the authors showed that removal of Stu2p resulted in less dynamic microtubules, by decreasing the catastrophe and rescue frequency without affecting the growth rate. How

does our in vitro data compare with the studies on dynamics in vivo in the absence of Stu2p? In vitro, we also saw a Stu2p-dependent increase in the catastrophe frequency consistent with the in vivo data. However, although Stu2p decreased the growth rate in vitro, no effect on the growth rate in the absence of Stu2p was noticed by Kosco et al. (2001). Several reasons can be imagined for this discrepancy. In vivo, Stu2p is operating in the context of other microtubule-associated proteins that influence microtubule dynamics, e.g., Bim1 or Bik1 (Berlin et al., 1990; Pellman et al., 1995; Tirnauer et al., 1999). As a comparison, XMAP215 depletion from cytoplasmic egg extracts does not drastically alter the growth rate, although it is a very potent effecter of growth rate in vitro (Gard and Kirschner, 1987; Vasquez et al., 1994; Tournebize et al., 2000). Most importantly, the microtubule-destabilizing activity of Stu2p might be regulated in a cell cycle–dependent manner in vivo. Cell cycle regulation could also account for the fact that in another in vivo study (Severin et al., 2001), based on its role in spindle elongation during anaphase, Stu2p was proposed to act as a microtubule stabilizer. An intriguing model that could reconcile the differences concerning the in vivo role of Stu2p is one in which Stu2p could change in a regulated manner from a stabilizer to a destabilizer.

The use of polarity-marked microtubules allowed us to demonstrate that the end binding of Stu2p is specific to plus ends, in agreement with in vivo data that showed Stu2p to be colocalized with microtubule ends of cytoplasmic microtubules (He et al., 2001; Kosco et al., 2001). Our results suggest that the binding of Stu2p to plus ends in vivo may be direct and not mediated through other proteins. Other end-binding proteins, such as Bim1 and Bik1, involved in attachment of microtubules to cortical sites have been suggested to interact with Stu2p (Chen et al., 1998; Miller et al., 2000; for review see Schuyler and Pellman, 2001). One possibility is that Stu2p binds to microtubule ends and recruits other end-binding factors. To our knowledge, Stu2p is the first described microtubule-associated protein that recognizes and binds specifically to the microtubule plus end in vitro. Other plus end binders, such as CLIP-170, have been described in the literature (Perez et al., 1999; for review see Schuyler and Pellman, 2001). However, these do not recognize microtubule ends directly but rather transiently associate with growing microtubule ends by copolymerization with tubulin (Diamantopoulos et al., 1999; for review see Schuyler and Pellman, 2001).

Materials and methods

Reaction buffers

Chemicals were from Sigma-Aldrich unless stated otherwise. The following reaction buffers were used: BRB80 (80 mM Pipes 6.8, 1 mM EGTA, 1 mM $MgCl_2$); SRB1 (BRB80, 80 mM KCl, 0.5 mg/ml casein, 1 mM GTP, 1 mM DTT); SRB2 (SRB1, 0.25% Brij-35); and SRB3 (BRB80, 100 mM KCl, 0.25% Brij-35, 5% glycerol).

Stu2p antibody production

Polyclonal Stu2p antibodies were raised against a COOH-terminal peptide of Stu2p in rabbits and subsequently affinity purified (Eurogentec).

Purification of tubulin and centrosomes

Tubulin was purified to homogeneity from porcine brain by three cycles of microtubule assembly before phosphocellulose chromatography (Ashford et al., 1998). Rhodamine or Oregon green labeling of tubulin was done as described previously (Hyman et al., 1991). Centrosomes were purified from human KE37 cells using a low ionic strength lysis step and subsequent sucrose gradients (Moudjou and Bornens, 1998).

Microtubule immunofluorescence

Microtubules were spotted at appropriate dilutions on poly-lysine microscope slides (Sigma-Aldrich), fixed for 3 min in −20°C methanol, and incubated in PBN (PBS, 2% BSA, 0.1% NP-40) for 5 min at RT. Microtubules were subsequently incubated directly with FITC-labeled DM1α tubulin antibody (Sigma-Aldrich) in PBN for 20 min at RT. After several washes, the slides were mounted in antifade-mounting medium. Images were acquired using a Axioplan 2 microscope (Carl Zeiss MicroImaging, Inc.) with a 63× Plan-Apochromat lens (NA 1.40; Carl Zeiss MicroImaging, Inc.) together with the MetaMorph Imaging System (version 1.4.2.) and processed using Adobe Photoshop®.

Preparation of yeast extracts

Yeast extracts were prepared in SRB3, 1 mM DTT, and protease inhibitor cocktail (Complete Mini, EDTA free; Roche) by bead beating using a W303 (mating type a) strain. Extracts were spun in a Beckman Coulter TLA 100 rotor at 100 krpm for 5 min at 4°C, and aliquots of the supernatant were snap frozen in liquid nitrogen and kept at −80°C. The protein concentration was between 10 and 20 mg/ml.

Purification of recombinant Stu2p as baculovirus-derived protein

A 500-ml suspension culture of Sf+ cells was infected at a density of 10^6 cells per ml with 2 ml of recombinant baculovirus at ~10^8 pfu/ml. Recombinant baculovirus expressing full-length Stu2p was a gift from Peter Sorger (Massachusetts Institute of Technology, Cambridge, MA) and prepared using the pFAST Bac system (Invitrogen). Cells were harvested 52 h after infection. Cell extracts were prepared by resuspension of the cell pellet in 50 mM Hepes, pH 7.5, 5% glycerol, 0.1% Triton X-100, 150 mM NaCl, and 1 mM DTT, and supplemented with protease inhibitors. The extracts, cleared by ultracentrifugation and ultrafiltration, were loaded onto a cation exchange column (HiTrap SP, 5 ml; Amersham Biosciences) equilibrated in CB (6.7 mM Hepes, 6.7 mM MES, 6.7 mM sodium acetate, pH 7.2) and 150 mM NaCl. A linear gradient from CB, 150 mM NaCl to CB, 1 M NaCl was developed over 10 column vol. Stu2p eluted between 420 and 490 mM NaCl. These fractions were pooled and run on a gel filtration column (Superose 6, prep grade; Amersham Biosciences) in BRB80, 75 mM KCl, 1 mM DTT, and 10 μM ATP, and supplemented with protease inhibitors. Fractions containing the Stu2p peak were pooled and loaded onto a cation exchange column (HiTrap SP, 1 ml; Amersham Biosciences), equilibrated, and run in BRB80, 100 mM KCl. Stu2p was eluted in BRB80, 450 mM KCl and desalted using a PD10 column equilibrated and run in SRB3 supplemented with protease inhibitors and (optionally) 0.25% Brij-35. This preparation was aliquoted, snap frozen, and kept in liquid nitrogen.

Direct labeling of Stu2p

7.5 μM recombinant Stu2p in SRB3 was incubated with 180 μM monoreactive Cy3 (Amersham Biosciences) for 1 h on ice. After quenching the reaction by addition of potassium glutamate to 220 mM, labeled Stu2p was desalted into SRB3 and spun at 100 krpm for 5 min at 4°C in a Beckman Coulter TLA 100 rotor. DTT was added to 1 mM, and the supernatant was aliquoted, snap frozen, and kept in liquid nitrogen. The labeling stoichiometry (dye to protein) was determined spectrophotometrically and found to be 1.05.

Gel filtration

Gel filtration was done on a Superose 6 PC 3.2/30 column (2.4 ml; Amersham Biosciences), equilibrated, and run in SRB3 at a flow rate of 0.02 ml/min. The column was calibrated in several runs with the following markers (Amersham Biosciences) of known Stokes radius: albumin, thyroglobulin, chymotrypsinogen A, ferritin, ovalbumin, catalase, aldolase, ribonuclease A. The void volume was determined using Blue Dextran. Recombinant Stu2p or yeast extracts cleared by ultrafiltration were subsequently run, 100-μl fractions were collected, and the peak position of Stu2p was determined using the chromatogram (absorption at 280 nm) or by SDS-PAGE and subsequent Western blotting of the collected fractions using a polyclonal Stu2p antibody.

Sucrose gradients

Sucrose step gradients were prepared from 5 to 40% sucrose (in SRB3) in five equal steps and allowed to diffuse into a linear gradient overnight at 4°C. Precleared (100 krpm in a Beckman Coulter TLA 100, at 4°C for 5 min) recombinant Stu2p or yeast extracts, and in parallel a mixture of BSA, aldolase, catalase, and thyroglobulin (Amersham Biosciences) as markers

of known S value, were spun through the gradients (4°C for 4 h at 50 krpm in a Beckman Coulter TLS 55 rotor), and gradients were fractionated by taking 16 equal fractions from the top. The position of proteins within the gradients was determined on Coomassie-stained SDS-PAGE gels (markers) or by Western blotting using a polyclonal Stu2p antibody (recombinant Stu2p and yeast extracts).

Microtubule nucleation assay

All protein preparations were precleared before usage (100 krpm in a Beckman Coulter TLA 100, at 4°C for 5 min). 22 μM tubulin was incubated in SRB2 with varying concentrations of Stu2p (0–2.5 μM) for 10 min at 29°C. Nucleated microtubules were separated from soluble tubulin by centrifugation through a 40% glycerol cushion (70 krpm for 5 min at 29°C in a Beckman Coulter TLA 100 rotor). Equivalent amounts of supernatant and pellet were analyzed by SDS-PAGE and Coomassie staining.

Determination of microtubule length by a fixed time point assay

Microtubules were grown from purified centrosomes at 26 μM tubulin (1:10 labeled with rhodamine tubulin) and various concentrations of Stu2p (0–1 μM Stu2p) in SRB2 at 29°C for 10 min. Prior to usage, protein preparations were precleared by centrifugation (100 krpm at 4°C for 5 min in a Beckman Coulter TLA 100 rotor). Reactions were fixed with 0.75% glutaraldehyde for 3 min and subsequently quenched for 5 min with 0.1% sodium borohydride. Part of the reaction was squashed under a coverslip and analyzed microscopically. Images were acquired using a Axioplan 2 Microscope (Carl Zeiss MicroImaging, Inc.) with a 63× Zeiss Plan-Apochromat lens (NA 1.40; Carl Zeiss MicroImaging, Inc.) together with the MetaMorph Imaging System (version 1.4.2.). The radii of at least 39 asters were measured for each Stu2p concentration using the MetaMorph Imaging software, and images were subsequently processed using Adobe Photoshop®.

Measurement of cytoplasmic microtubule length in vivo

Wild-type cells or stu2–10 cells (both GFP-tub1–His3 and derivatives of W303) were grown in YP, 2% raffinose at 25°C to an OD_{600} of 0.4, arrested with 100 mM HU at 25°C for 140 min, and shifted to 37°C for another 140 min. A FACScan® was used as described (Epstein and Cross, 1992). Cells were prepared for indirect immunofluorescence as published (Piatti et al., 1996) using the mouse monoclonal antitubulin antibody DM1α (Sigma-Aldrich) and a FITC-conjugated secondary antibody. DNA was visualized by DAPI. Imaging was done using a 100×, 1.35 NA objective on an Olympus DeltaVision microscope using SoftWorx (Applied Precision). 40 0.2-μm stacks were taken for each field, and cytoplasmic microtubule length in single cells was measured three-dimensionally from the tip of the microtubule to the spindle pole body as multiple segments (SoftWorx; Applied Precision). Between 153 and 175 cytoplasmic microtubules were quantitated. Images depicted in this paper were projected using SoftWorx (Applied Precision) and processed using Adobe Photoshop®. To determine cell sizes, DIC images of at least 68 cells were acquired using a Axioplan 2 microscope (Carl Zeiss MicroImaging, Inc.) with a 63× Plan-Apochromat lens (NA 1.40; Carl Zeiss MicroImaging, Inc.) together with the MetaMorph Imaging System (version 1.4.2.). Cells were analyzed by measuring the length of a line drawn from the tip of the mother cell through the bud neck to the tip of the bud using the MetaMorph Imaging software. The average mother cell–bud distance was for the cells arrested at the permissive temperature with HU before the shift to the restrictive temperature: 6.5 ± 1.1 μm (standard deviation) for the wild-type and 6.5 ± 1.0 μm for the stu2–10 cells. After the temperature shift, this distance was 7.5 ± 1.1 μm for the wild-type and 7.5 ± 1.1 μm for the stu2–10 cells. Thus, stu2–10 and wild-type cells did not differ in their size.

VE-DIC

The VE-DIC assay was adapted from Kinoshita et al. (2001). Small (~12 μl) home made perfusion chambers were put on a metal block on ice, and purified centrosomes were perfused into the chambers and allowed to adsorb to the coverslips for 5 min. The glass surface was blocked three times for 5 min with 5 mg/ml casein in BRB80, and free casein was removed by four washes with 20 μl 0.25% Brij-35 in BRB80. 30-μl mixtures of prespun (4°C for 5 min at 100 krpm in a Beckman Coulter TLA 100 rotor) tubulin (21.5 μM) and various levels of prespun Stu2p (0–1 μM) in SRB2 was perfused at 4°C into the chambers. Reactions were started by transferring the chambers to a metal block at RT and then immediately onto the stage of a VE-DIC microscope kept in a temperature control box at 29°C. For each experiment, one aster was analyzed between 5 and 12 min after the start of the reaction. At least four experiments were done at each concentration of Stu2p. Videos were acquired on an Olympus BX50 microscope using an Olympus PlanApo 60× lens (NA 1.40) and a Hamamatsu 2400 Newvicon video-camera. Images were enhanced with an Argus 20 (Hamamatsu). Microtubules were tracked using ScionImage (version 1.62). The parameters of microtubule polymerization were subsequently determined from the entire dataset at each concentration of Stu2p. Rescue events occurred too rarely to be reported as a rescue frequency.

To determine the relationship of growth rate to catastrophe frequency, we used the same set-up with minor changes: smaller chambers (~6 μl) were employed and axonemes (gifts from Denis Chrétien, Université de Rennes, Rennes, France) instead of centrosomes were used as microtubule nucleators. The tubulin concentration ranged from 14.3 to 27.5 μM in SRB2. Three films from ~1.5 to ~13 min after the start of the reaction were obtained at each concentration of tubulin. Microtubule growth rates were linear with tubulin concentration. Microtubules were grouped according to their growth rates in groups of 0.06-μm/min increments, and the average growth rate and the catastrophe frequency of the groups were subsequently calculated. Groups contained between 9 microtubules with a total growth time of 19 min and 44 microtubules with a total growth time of 104 min.

Microtubule shearing

Taxol-stabilized microtubules were sheared on ice 10 times for 1 s with 3 min on ice in between with a tip sonicator at 40% amplitude. The lengths of at least 91 microtubules were determined by immunofluorescence using the MetaMorph Imaging software. The average microtubule length was 16.6 μm for the unsheared (SEM [$P < 0.05$]; 2.5 μm) and 3.4 μm for the sheared microtubules (SEM [$P < 0.05$]; 0.5 μm).

Microtubule copelleting assay

Increasing amounts of taxol-stabilized microtubules were incubated in SRB2: 20 μM taxol with prespun (4°C for 5 min at 100 krpm in a Beckman Coulter TLA 100 rotor) Stu2p for 5 min at RT. Microtubule-bound protein was separated from unbound protein by centrifugation (25°C for 5 min at 70 krpm in a Beckman Coulter TLA 100 rotor). For the shearing experiment, the reactions were spun through a 40% glycerol BRB80 cushion. Equivalent amounts of supernatants and pellets were subsequently analyzed by Western blotting using a polyclonal Stu2p antibody, the monoclonal anti–α-tubulin antibody DM1α (Sigma-Aldrich), or the monoclonal anti–β-tubulin antibody TUB2.1 (Sigma-Aldrich). The percentage of binding was measured using the Histogram function in Adobe Photoshop®.

Production of polarity-marked microtubules

Bright microtubule seeds were made by incubating 75 μM of a prespun (4°C for 5 min at 100 krpm in a Beckman Coulter TLA 100 rotor) 1.8:1 mixture of Oregon green–labeled tubulin and unlabeled tubulin in BRB80, 1 mM DTT with 0.1 mM GMPCPP at 37°C for 15 min. The seeds were diluted 1:125 in a prewarmed mixture containing 20 μM of a 1:5 mixture of Oregon green–labeled and unlabeled tubulin in BRBR80, 1 mM GTP, 1 mM DTT, and 12.5 μM NEM-treated tubulin (to inhibit minus end polymerization). After a 30-min incubation at 37°C, the mixture was diluted in prewarmed BRB80, 20 μM taxol, and 1 mM DTT. Taxol-stabilized microtubules were reconcentrated by centrifugation (25°C for 5 min at 50 krpm in a Beckman Coulter TLA 100 rotor) and resuspended in BRB80, 20 μM taxol, and 1 mM DTT.

Removal of the COOH terminus of β-tubulin in microtubules

Taxol-stabilized microtubules were incubated in BRB80, 1 mM DTT, and 20 μM taxol for 15 min at 37°C with 30 μg/ml subtilisin (Fluka). The digestion was stopped by adding PMSF to 5 mM. Completion of digestion was checked by SDS-PAGE and Coomassie staining or by Western blotting using the β-tubulin–specific mAb TUB2.1 (Sigma-Aldrich) whose epitope is situated in the COOH terminus of β-tubulin.

Visualization of Stu2p binding on microtubules

Prespun (4°C for 5 min at 100 krpm in a Beckman Coulter TLA100 rotor) 16 nM directly labeled Stu2p in SRB3, 1 mM DTT, and 20 μM taxol was incubated for 5 min at RT with 11.5 μM taxol-stabilized polarity marked microtubules. The reaction was fixed with 0.75% glutaraldehyde for 3 min, quenched for 5 min with 0.1% sodium borohydride, and analyzed microscopically after a 1:200 dilution in SRB3, 20 μM taxol. Images were acquired using a Axioplan 2 microscope with a 63× Plan-Apochromat lens (NA 1.40; Carl Zeiss MicroImaging, Inc.) together with the MetaMorph Imaging System (version 1.4.2.). The intensities of the signals in the rhodamine (Stu2p) channel were scanned along the length of microtubules using the Linescan function of the MetaMorph Imaging software with a pixel width of 5. Peaks higher then 10% of the median intensity along the microtubule were scored with their location along the microtubule. Microtubules were divided in 10% intervals from their minus ends to their plus ends. 124 polarity marked microtubules were quantitated. In the absence of directly labeled Stu2p, no significant number of peaks were detected. The median intensity in the absence and presence of directly labeled Stu2p was found to be virtually identical. Images were processed using Adobe Photoshop®.

Online supplemental material

Fig. S1 demonstrates that Stu2p interacts with itself in vivo. The figure is available online at http://www.jcb.org/cgi/content/full/jcb.200211097/DC1.

We acknowledge Peter Sorger for the kind gift of recombinant baculovirus, Denis Chrétien for the kind gift of axonemes, Susi Berthold for the help with expressing and purifying Stu2p, and the members of the Hyman lab for their comments on this manuscript.

Submitted: 21 November 2002
Revised: 12 February 2003
Accepted: 12 February 2003

References

Akhmanova, A., C.C. Hoogenraad, K. Drabek, T. Stepanova, B. Dortland, T. Verkerk, W. Vermeulen, B.M. Burgering, C.I. De Zeeuw, F. Grosveld, and N. Galjart. 2001. Clasps are CLIP-115 and -170 associating proteins involved in the regional regulation of microtubule dynamics in motile fibroblasts. *Cell.* 104:923–935.

Arnal, I., E. Karsenti, and A. Hyman. 2000. Structural transitions at microtubule ends correlate with their dynamic properties in *Xenopus* egg extracts. *J. Cell Biol.* 149:767–774.

Ashford, A., S.S.L. Andersen, and A. Hyman. 1998. Preparation of tubulin from bovine brain. *In* Cell Biology: A Laboratory Handbook. 2nd edition. Vol. 2. Julio E. Cells, editor. Academic Press, Inc., Orlando, FL. 205–212.

Belmont, L., and T. Mitchison. 1996. Identification of a protein that interacts with tubulin dimers and increases the catastrophe rates of microtubules. *Cell.* 84: 623–631.

Berlin, V., C.A. Styles, and G.R. Fink. 1990. BIK1, a protein required for microtubule function during mating and mitosis in *Saccharomyces cerevisiae*, colocalizes with tubulin. *J. Cell Biol.* 111:2573–2586.

Brunner, D., and P. Nurse. 2000. CLIP170-like tip1p spatially organizes microtubular dynamics in fission yeast. *Cell.* 102:695–704.

Cassimeris, L., D. Gard, P.T. Tran, and H.P. Erickson. 2001. XMAP215 is a long thin molecule that does not increase microtubule stiffness. *J. Cell Sci.* 114: 3025–3033.

Chen, X.P., H. Yin, and T.C. Huffaker. 1998. The yeast spindle pole body component Spc72p interacts with Stu2p and is required for proper microtubule assembly. *J. Cell Biol.* 141:1169–1179.

Chretien, D., S.D. Fuller, and E. Karsenti. 1995. Structure of growing microtubule ends: two-dimensional sheets close into tubes at variable rates. *J. Cell Biol.* 129:1311–1328.

Cullen, C.F., P. Deak, D.M. Glover, and H. Ohkura. 1999. Mini spindles: a gene encoding a conserved microtubule-associated protein required for the integrity of the mitotic spindle in *Drosophila*. *J. Cell Biol.* 146:1005–1018.

Curmi, P.A., S.S.L. Andersen, S. Lachkar, O. Gavet, E. Karsenti, M. Knossow, and A. Sobel. 1997. The Stathmin/tubulin interaction in vitro. *J. Biol. Chem.* 272:25029–25036.

Davis, L.J., D.J. Odde, S.M. Block, and S.P. Gross. 2002. The importance of lattice defects in katanin-mediated microtubule severing in vitro. *Biophys. J.* 82: 2916–2927.

Desai, A., and T.J. Mitchison. 1997. Microtubule polymerization dynamics. *Annu. Rev. Cell Dev. Biol.* 13:83–117.

Desai, A., S. Verma, T.J. Mitchison, and C.E. Walczak. 1999. Kin I kinesins are microtubule-destabilizing enzymes. *Cell.* 96:69–78.

Diamantopoulos, G.S., F. Perez, H.V. Goodson, G. Batelier, R. Melki, T.E. Kreis, and J.E. Rickard. 1999. Dynamic localization of CLIP-170 to microtubule plus ends is coupled to microtubule assembly. *J. Cell Biol.* 144:99–112.

Drechsel, D.N., A.A. Hyman, M.H. Cobb, and M.W. Kirschner. 1992. Modulation of the dynamic instability of tubulin assembly by the microtubule-associated protein tau. *Mol. Biol. Cell.* 3:1141–1154.

Epstein, C.B, and F.R. Cross. 1992. CLB5: a novel B cyclin from budding yeast with a role in S phase. *Genes Dev.* 69:1695–1706.

Gard, D.L., and M.W. Kirschner. 1987. A microtubule-associated protein from *Xenopus* eggs that specifically promotes assembly at the plus-end. *J. Cell Biol.* 105:2203–2215.

He, X., D.R. Rines, C.W. Espelin, and P.K. Sorger. 2001. Molecular analysis of kinetochore-microtubule attachment in budding yeast. *Cell.* 106:195–206.

Howell, B., N. Larsson, M. Gullberg, and L. Cassimeris. 1999. Dissociation of the tubulin-sequestering and microtubule catastrophe-promoting activities of oncoprotein18/stathmin. *Mol. Biol. Cell.* 10:105–118.

Hyman, A., D. Drechsel, D. Kellogg, S. Salser, K. Sawin, P. Steffen, L. Wordeman, and T. Mitchison. 1991. Preparation of modified tubulins. *Methods Enzymol.* 196:478–485.

Jourdain, L., P. Curmi, A. Sobel, D. Pantaloni, and M.F. Carlier. 1997. Stathmin: a tubulin-sequestering protein which forms a ternary T_2S complex with two tubulin molecules. *Biochemistry.* 36:10817–10821.

Kinoshita, K., I. Arnal, A. Desai, D.N. Drechsel, and A.A. Hyman. 2001. Reconstitution of physiological microtubule dynamics using purified components. *Science.* 294:1340–1343.

Kinoshita, K., B. Habermann, and A. Hyman. 2002. XMAP215: a key component of the dynamic microtubule cytoskeleton. *Trends Cell Biol.* 12:267–273.

Kosco, K.A., C.G. Pearson, P.S. Maddox, P.J. Wang, I.R. Adams, E.D. Salmon, K. Bloom, and T.C. Huffaker. 2001. Control of microtubule dynamics by Stu2p is essential for spindle orientation and metaphase chromosome alignment in yeast. *Mol. Biol. Cell.* 12:2870–2880.

Lee, M.J., F. Gergely, K. Jeffers, S.Y. Peak-Chew, and J.W. Raff. 2001. Msps/XMAP215 interacts with the centrosomal protein D-TACC to regulate microtubule behaviour. *Nat. Cell Biol.* 3:643–649.

Matthews, L.R., P. Carter, D. Thierry-Mieg, and K. Kemphues. 1998. ZYG-9, A *Caenorhabditis elegans* protein required for microtubule organization and function is a component of meiotic and mitotic spindle poles. *J. Cell Biol.* 141:1159–1168.

McNally, F.J., and R.D. Vale. 1993. Identification of katanin, an ATPase that severs and disassembles stable microtubules. *Cell.* 75:419–429.

Miller, R.K., S.C. Cheng, and M.D. Rose. 2000. Bim1p/Yeb1p mediates the Kar9p-dependent cortical attachment of cytoplasmic microtubules. *Mol. Biol. Cell.* 11:2949–2959.

Moores, C.A., M. Yu, J. Guo, C. Beraud, R. Sakowicz and R.A. Milligan. 2002. A mechanism for microtubule depolymerization by KinI kinesins. *Mol. Cell.* 94:903–909.

Moudjou, M., and M. Bornens. 1998. Method of centrosome isolation from cultured animal cells. *In* Cell Biology: A Laboratory Handbook, 2nd edition. Vol. 2. Julio E. Cells, editor. Academic Press, Inc., Orlando, FL. 111–119.

Nakamura, M., X.Z. Zhou, and K.P. Lu. 2001. Critical role for the EB1 and APC interaction in the regulation of microtubule polymerization. *Curr. Biol.* 11: 1062–1067.

Ohkura, H., M.A. Garcia, and T. Toda. 2001. Dis1/TOG universal microtubule adaptors—one MAP for all? *J. Cell Sci.* 114:3805–3812.

Pellman, D., M. Bagget, Y.H. Tu, G.R. Fink, and H. Tu. 1995. Two microtubule-associated proteins required for anaphase spindle movement in *Saccharomyces cerevisiae*. *J. Cell Biol.* 130:1373–1385.

Perez, F., G.S. Diamantopoulos, R. Stalder, and T.E. Kreis. 1999. CLIP-170 highlights growing microtubule ends in vivo. *Cell.* 96:517–527.

Piatti, S., T. Bohm, J.H. Cocker, J.F. Diffley, and K. Nasmyth. 1996. Activation of S-phase–promoting CDKs in late G1 defines a "point of no return" after which Cdc6 synthesis cannot promote DNA replication in yeast. *Genes Dev.* 10:1516–1531.

Popov, A.V., A. Pozniakovsky, I. Arnal, C. Antony, A.J. Ashford, K. Kinoshita, R. Tournebize, A.A. Hyman, and E. Karsenti. 2001. XMAP215 regulates microtubule dynamics through two distinct domains. *EMBO J.* 20:397–410.

Popov, A., F. Severin, and E. Karsenti. 2002. XMAP215 is required for the microtubule-nucleating activity of centrosomes. *Curr. Biol.* 12:1326–1330.

Schuyler, S.C., and D. Pellman. 2001. Microtubule "plus-end-tracking proteins": the end is just the beginning. *Cell.* 105:421–424.

Serrano, L., E. Montejo de Garcini, M.A. Hernandez, and J. Avila. 1985. Localization of the tubulin binding site for tau protein. *Eur. J. Biochem.* 153:595–600.

Severin, F., B. Habermann, T. Huffaker, and T. Hyman. 2001. Stu2p promotes mitotic spindle elongation in anaphase. *J. Cell Biol.* 153:435–442.

Spittle, C., S. Charrasse, C. Larroque, and L. Cassimeris. 2000. The interaction of TOGp with microtubules and tubulin. *J. Biol. Chem.* 275:20748–20753.

Tirnauer, J.S., E. O'Toole, L. Berrueta, B.E. Bierer, and D. Pellman. 1999. Yeast Bim1p promotes the G1-specific dynamics of microtubules. *J. Cell Biol.* 145:993–1007.

Tournebize, R., A. Popov, K. Kinoshita, A.J. Ashford, S. Rybina, A. Pozniakovsky, T.U. Mayer, C.E. Walczak, E. Karsenti, and A.A. Hyman. 2000. Control of microtubule dynamics by the antagonistic activities of XMAP215 and XKCM1 in *Xenopus* egg extracts. *Nat. Cell Biol.* 2:13–19.

Vasquez, R.J., D.L. Gard, and L. Cassimeris. 1994. XMAP from *Xenopus* eggs promotes rapid plus end assembly of microtubules and rapid microtubule turnover. *J. Cell Biol.* 127:985–993.

Wang, P.J., and T.C. Huffaker. 1997. Stu2p: a microtubule-binding protein that is an essential component of the yeast spindle pole body. *J. Cell Biol.* 139:1271–1280.